FEBS Letters 584 (2010) 1521–1525

FEBS Letters

journal homepage: www.FEBSLetters.org

QSOX contains a pseudo-dimer of functional and degenerate sulfhydryl oxidase domains

Assaf Alon [a], Erin J. Heckler [b], Colin Thorpe [b], Deborah Fass [a,*]

[a] Department of Structural Biology, Weizmann Institute of Science, Rehovot 76100, Israel
[b] Department of Chemistry and Biochemistry, University of Delaware, Newark, Delaware 19716, USA

ARTICLE INFO

Article history:
Received 31 January 2010
Revised 2 March 2010
Accepted 2 March 2010
Available online 6 March 2010

Edited by Kaspar Locher

Keywords:
Disulfide bond formation
Domain duplication
Domain fusion
Flavin adenine dinucleotide
Sulfhydryl oxidase

ABSTRACT

Quiescin sulfhydryl oxidase (QSOX) catalyzes formation of disulfide bonds between cysteine residues in substrate proteins. Human QSOX1 is a multi-domain, monomeric enzyme containing a module related to the single-domain sulfhydryl oxidases of the Erv family. A partial QSOX1 crystal structure reveals a single-chain pseudo-dimer mimicking the quaternary structure of Erv enzymes. However, one pseudo-dimer "subunit" has lost its cofactor and catalytic activity. In QSOX evolution, a further concatenation to a member of the protein disulfide isomerase family resulted in an enzyme capable of both disulfide formation and efficient transfer to substrate proteins.

1. Introduction

Disulfide bond formation in proteins that enter the endoplasmic reticulum (ER) is catalyzed by the sulfhydryl oxidase Endoplasmic reticulum oxidoreductin 1 (Ero1) and the dithiol/disulfide oxidoreductase protein disulfide isomerase (PDI), both highly conserved from yeast to humans [1–3]. In metazoans, plants, and certain protists, however, secretory proteins may encounter another sulfhydryl oxidase downstream of Ero1. This additional catalyst of disulfide formation is known as Quiescin Sulfhydryl OXidase (QSOX) because its transcript levels increase as cultured cells reach confluence and enter a quiescent state [4,5]. Interest in QSOX is intensifying, due in part to its abnormal expression in pancreatic [6], prostate [7], and perhaps other cancers.

Although a definitive biological role and substrate set have yet to be described for QSOX, much is known about mammalian QSOX localization on the cellular and tissue levels. QSOX is found predominantly in the Golgi, in secretory granules, and secreted from cells [8–10], though it has also been detected in the endoplasmic reticulum [8]. QSOX is expressed most strongly in cell types with high secretory loads in the immune, neural, reproductive, respiratory, and digestive systems, as well as in the skin and retina (reviewed in [11]). The presence of QSOX later in the secretory pathway than Ero1 suggests that its primary role may be to cross-link higher order assemblies of structural proteins, such as those of the extracellular matrix, rather than to introduce disulfides into individual proteins early in oxidative folding. However, the list of possible QSOX targets remains hypothetical [12].

Based on amino acid sequence analyses [5] and protein dissection [13], QSOX was found to be a fusion of two functional modules (Fig. 1). At the amino terminus, QSOX contains a dithiol/disulfide oxidoreductase module related to PDI. Toward its carboxy-terminus QSOX has a sulfhydryl oxidase module, which forms disulfides de novo. Though QSOX thus encompasses the functions of both Ero1 and PDI, its sulfhydryl oxidase domain is not related to Ero1 but rather to a distinct enzyme family found primarily in mitochondria [14] and in the cytosol of certain virally infected cells [15]. This family is known as the Erv sulfhydryl oxidases because the yeast mitochondrial version is *e*ssential for *r*espiration and *v*iability.

The first QSOX enzyme studied in depth biochemically, purified from chicken eggs [16–18], was shown by size exclusion chromatography to be dimeric [16]. As all Erv enzymes studied to date are also dimers [19–22], it was reasonable to hypothesize that QSOX enzymes might all be dimers that self-associate through their Erv-like domains. However, a recent study of recombinant human QSOX1 (HsQSOX1) [23] confirmed earlier experiments on

* Corresponding author. Fax: +972 8 934 4136.
E-mail address: deborah.fass@weizmann.ac.il (D. Fass).

0014-5793/$36.00
doi:10.1016/j.febslet.2010.03.001

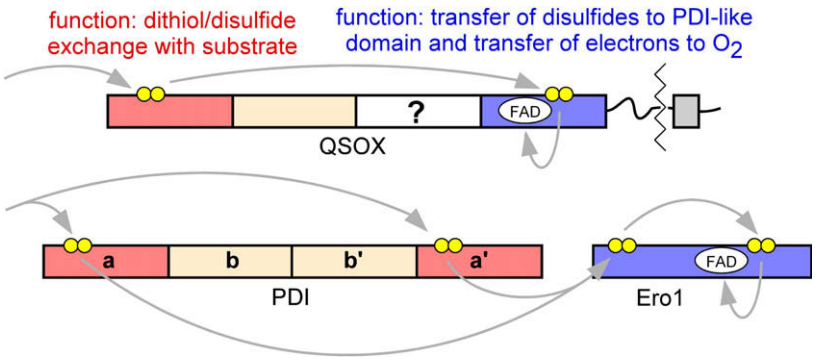

Fig. 1. Schematic diagram illustrating the domain composition of QSOX compared to the Ero1/PDI pair, which catalyze the introduction of disulfide bonds into proteins in the endoplasmic reticulum. Sulfhydryl oxidase domains and a description of their function are in blue. Thioredoxin fold domains are shown in pink, with the catalytically active subset in a darker shade. The lettering on the PDI domains is the standard nomenclature for thioredoxin fold domains within this enzyme. The question mark in QSOX corresponds to the helix-rich region (HRR). Redox-active disulfides are illustrated as pairs of yellow balls; other disulfides in the proteins are omitted from this presentation. The QSOX transmembrane region is shown as a grey box, with the jagged line indicating that alternative splicing yields a version without the transmembrane segment. Gray arrows show the proposed two-electron transfer steps involved in catalyzing disulfide bond formation and transfer in the QSOX and Ero1/PDI systems. The relative extent to which the **a** and **a′** domains of PDI serve as physiological electron donors to Ero1 may differ in different organisms.

endogenous material from rat seminal vesicles [24] showing mammalian QSOX to be monomeric. This finding raised questions regarding the pathway for electron transport within the enzyme [23]. Clearly, a greater understanding of the domain organization of QSOX, and the relative positions of its redox-active sites, would facilitate interpretation of biochemical experiments and the design of studies to probe the physiological roles and substrates of this complex disulfide-generating catalyst. We present here the first structural study of a QSOX enzyme. Crystallization of a HsQSOX1 fragment containing the sulfhydryl oxidase active site resolves the apparent contradiction between dimerization of single-domain Erv enzymes and the monomeric state of mammalian QSOX.

2. Materials and methods

2.1. Vector construction and protein expression

The region of the human QSOX1 gene encoding amino acids 33–546 was introduced into the pET-15b vector (Novagen) between the Nde I and Bam HI restriction sites. The segment between the Nco I and Nde I sites of the resulting construct was replaced using synthetic oligonucleotides to eliminate the thrombin cleavage site and incorporate a His_6 tag fused directly to the protein. The sequence AAAENLYFQSAAA, including A TEV protease cleavage site (underlined), was inserted in place of the original sequence EAA at positions 272–274. The replacement was accomplished by mutation to introduce a Not I restriction site, followed by cleavage at the Not I site and ligation of synthetic oligonucleotides encoding the desired sequence. Although a carboxy-terminal fragment of HsQSOX could also be expressed directly, material derived from protease cleavage of the larger HsQSOX construct yielded the crystals used for data collection.

2.2. Protein expression and purification

The recombinant QSOX construct $HsQSOX1_{33–546}$ including the inserted TEV cleavage site was expressed in the *Escherichia coli* strain BL21 (DE3) plysS (Novagen). Cells were grown in LB containing 100 mg/l ampicillin and 30 mg/l chloramphenicol to an $OD_{600\ nm}$ of 0.5–0.6 at 37 °C. Isopropyl-1-thio-β-D-galactopyranoside was added to a final concentration of 0.5 mM, and the cultures were grown for a further 36 h at 15 °C. Cells were harvested and suspended in 20 mM sodium phosphate buffer, 500 mM NaCl, and 20 mM imidazole (pH 7.4), sonicated on ice, and centrifuged for 1 h at 40 000×*g*. The supernatant was applied to a 5 ml Ni-NTA column using an AKTA FPLC (both from GE Healthcare), and protein was eluted in 20 mM sodium phosphate buffer, 500 mM NaCl, and a gradient of imidazole (20–500 mM) (pH 7.4). Eluted protein was dialyzed overnight into 20 mM sodium phosphate buffer, 200 mM NaCl (pH 7.4). TEV protease was expressed from a plasmid provided by David Waugh (National Cancer Institute) and purified using Ni-NTA chromatography. TEV cleavage of $HsQSOX1_{33–546}$ was performed at room temperature for 6 h. Following cleavage, protein solution was again applied to a Ni-NTA column. The $HsQSOX1_{273–546}$ fragment did not bind the column and was collected and dialyzed against 20 mM Tris, 200 mM NaCl (pH 8.0). Limited proteolysis at a concentration of 0.5 mg/ml $HsQSOX1_{273–546}$ was performed for 1 hr at room temperature using a 1:250 w/w ratio of trypsin:QSOX. Cleavage was terminated by addition of phenylmethanesulfonyl fluoride to a concentration of 1 mM. MALDI-TOF mass spectrometry of the resulting material yielded a mass of 29 742 Da. The calculated mass of $HsQSOX1_{286–546}$ is 29 741.4 after subtraction of 6 Da due to three disulfides, consistent with $HsQSOX1_{286–546}$ being the product of trypsin digestion. $HsQSOX1_{286–546}$ was subjected to gel filtration, and peak fractions were pooled and concentrated to 25 mg/ml. The selenomethionine variant was expressed according to published protocol [25] and processed as described for wild-type $HsQSOX1_{286–546}$.

2.3. Crystallization, data collection, and structure refinement

Crystals of $HsQSOX1_{286–546}$ in space group $P6_422$ were grown by hanging drop vapor diffusion over well solution containing 100 mM citric acid (pH 5.3–5.6) and 12–16% (w/v) PEG 8000. Microseeding into the same conditions gave larger crystals. Adding 10–15% ethanol to the well solution occasionally yielded crystals of space group C222. Crystals were transferred to a 1:1 mixture of Paratone oil (Exxon) and mineral oil before flash-freezing. Data were collected from a C222 crystal at 100 K on a RU-H3R generator (Rigaku, Tokyo) equipped with a RaxisIV image plate and Osmic mirrors. MAD data were collected from a $P6_422$ crystal at the ID-29 beamline at the European Synchrotron Radiation Facility (ESRF), Grenoble, France. Data were processed and scaled using DENZO and SCALEPACK [26]. Heavy atom site identification and phasing were performed using PHENIX [27], and an initial model was built using Coot [28]. PHASER [29] was then used to solve the C222 crystals by molecular replacement. Structure models were refined using CNS [30]. Data collection and refinement statistics are reported in Table 1.

Table 1
Crystallographic and refinement statistics.

Space group	$P6_422$ native	$P6_422$ Semet peak	$P6_422$ Semet remote	$P6_422$ Semet inflection	C222 native
Unit cell parameters (Å)	85.61 × 85.61 × 125.71; $\alpha = \beta = 90°$, $\gamma = 120°$	85.65 × 85.65 × 125.76; $\alpha = \beta = 90°$, $\gamma = 120°$	85.69 × 85.69 × 125.84; $\alpha = \beta = 90°$, $\gamma = 120°$	85.68 × 85.68 × 125.80; $\alpha = \beta = 90°$, $\gamma = 120°$	83.48 × 161.57 × 121.94; $\alpha = \beta = \gamma = 90°$
Resolution[a] (Å)	50–2.05 (2.12–2.05)	50–2.0 (2.03–2.00)	50–2.0 (2.03–2.00)	50–2.0 (2.03–2.00)	50–2.0 (2.07–2.00)
Completeness (%)	99.8 (98.1)	96.2 (98.5)	95.9 (98.1)	96.2 (98.4)	98.8 (100)
Redundancy	16.0 (11.3)	11.8 (12.2)	11.9 (12.2)	11.9 (12.1)	5.9 (5.8)
R_{sym}[b]	0.056 (0.737)	0.079 (0.867)	0.074 (0.562)	0.084 (0.968)	0.065 (0.553)
$R_{p.i.m}$[c]	0.014 (0.189)	0.026 (0.255)	0.024 (0.313)	0.026 (0.286)	
$\langle I/\sigma I \rangle$	16.4 (2.6)	11.0 (4.0)	12.5 (3.2)	10.9 (3.4)	12.6 (2.9)
Number of heavy atom sites		3			
Figure of merit for phasing (to 2.0 Å)		0.458 (0.631 after density modification)			

Refinement statistics	$P6_422$	C222
Protein molecules per asymmetric unit	1	3
Total reflections/test set	17681/1207	55254/3928
R_{work}/R_{free}[d]	0.275/0.324	0.237/0.271
Rms deviations from ideality		
Bonds (Å)	0.011	0.007
Angles (°)	1.725	2.184
Number of atoms		
Protein	2023	5853
Water	103	452
FAD	53	159
Citrate	–	13

[a] Numbers in parentheses are for the highest resolution bin.
[b] $R_{sym} = \Sigma_{hkl}\Sigma_i|I_i(hkl) - \langle I(hkl)\rangle|/\Sigma_{hkl}\Sigma_i I_i(hkl)$, where $I_i(hkl)$ is the observed intensity and $\langle I(hkl)\rangle$ is the average intensity for i observations.
[c] $R_{p.i.m.} = \Sigma_{hkl}[1/(N-1)]^{1/2}\Sigma_i|I_i(hkl) - \langle I(hkl)\rangle|/\Sigma_{hkl}\Sigma_i I_i(hkl)$ as described for the precision-indicating merging R factor [33]. Values were calculated using the program RMERGE (available at http://www.embl-hamburg.de/~msweiss/projects/msw_qual.html).
[d] R_{work}, $R_{free} = \Sigma||F_{obs}| - |F_{calc}||/\Sigma|F_{obs}|$, where F_{obs} and F_{calc} are the observed and calculated structure factors, respectively. A set of reflections (6.8% for $P6_422$ and 7.1% for C222) were excluded from refinement and used to calculate R_{free}.

3. Results

3.1. Expression of the sulfhydryl oxidase fragment of HsQSOX1

The folds of three HsQSOX1 domains can be classified by amino acid sequence analyses (Fig. 1). The amino-terminal domain shows 30–35% sequence identity to various PDI family members. The second domain of HsQSOX1, though highly diverged and lacking a Cys-X-X-Cys redox-active motif, is identified by fold-recognition algorithms as a thioredoxin superfamily domain (not shown). The third recognizable HsQSOX1 domain, toward the carboxy-terminus, is related to the Erv family of flavin adenine dinucleotide (FAD)-dependent sulfhydryl oxidases and contains conserved motifs involved in FAD binding and disulfide formation [31]. The remaining region of HsQSOX1, between the catalytically inactive thioredoxin fold domain and the Erv family module (question mark in Fig. 1), is predicted to have high helix content, but this helix-rich region (HRR) does not show sequence similarity with any other known protein.

The unique modification of a PDI family member by fusion to a catalyst of de novo disulfide formation motivates an investigation into the manner in which the HsQSOX1 domains interact to coordinate disulfide formation and transfer. To determine the context of the disulfide-generating module within the multi-domain HsQSOX1 structure, we isolated and crystallized a HsQSOX1 fragment spanning the HRR and Erv regions. HsQSOX1, like chicken QSOX [13], has a protease-sensitive region immediately downstream of the redox-inactive thioredoxin fold domain. Into this region we inserted a TEV protease site to facilitate specific cleavage and isolation of the carboxy-terminal HsQSOX1 fragment. Additional proteolytic trimming resulted in a fragment named $HsQSOX1_{286–546}$ according to its amino acid boundaries.

3.2. Structure of the $HsQSOX1_{286–546}$ Erv domain

The structure of the HsQSOX fragment containing the sulfhydryl oxidase domain was determined by X-ray crystallography to 2.0 Å resolution and is presented in Fig. 2A, in comparison with a single-domain Erv family protein. Independent copies of $HsQSOX1_{286–546}$ showed similar conformations (Fig. 2B), with a largest pair-wise root-mean-square deviation for Cα positions of 0.6 Å for all four molecules in the two crystal forms. As predicted, the Erv domain of HsQSOX1 shares the same fold as single-domain members of the family (Fig. 2A) and binds FAD similarly at the mouth of a slightly funnel-shaped four-helix bundle (Fig. 2C).

One significant difference between the QSOX FAD binding domain and previously determined Erv family structures is that the active site within the $HsQSOX1_{286–546}$ fragment appears to be sterically more accessible (Fig. 2C). Helix α1 of other Erv proteins are a turn or two longer at their amino-termini than helix α1 of $HsQSOX1_{286–546}$. The region just amino-terminal to helix α1 in HsQSOX consists of the disulfide-bonded loop between Cys393 and Cys405, and this loop is more distant from the active-site cysteines than are the amino-terminal ends of typical Erv α1 helices. $HsQSOX1_{286–546}$ lacks the basic residue that projects in other Erv enzymes from helix α1 into the vicinity of the active-site disulfide (Fig. 2C) and is presumably important in stabilizing the reduced, thiolate form of an active-site cysteine [31].

The FAD binding domain of QSOX further differs from other Erv enzymes in the locations of non-active-site disulfide bonds. First, a $CX_{16}C$ structural disulfide linking helix α4 with the following loop in mitochondrial Erv enzymes is absent in QSOX (Fig. 2A). Second, sequence alignments would suggest that the most carboxy-terminal QSOX disulfide, a highly conserved CXXC motif, corresponds to the Erv "shuttle" disulfide, which mediates transfer of electrons from substrate to the FAD-proximal, active-site cysteines [19]. However, there is a discrepancy of ~20 Å in the positions of the QSOX CXXC and Erv shuttle cysteines in structure superpositions. Due to two extra HsQSOX1 loops with no counterparts in other Erv enzymes, the QSOX disulfide in question is located amino-terminal rather than carboxy-terminal to helix α5 (Fig. 2A). These two extra HsQSOX1 loops are the ~10 residue segment (residues 490–500) immediately downstream of helix α4 and a ~20 residue loop

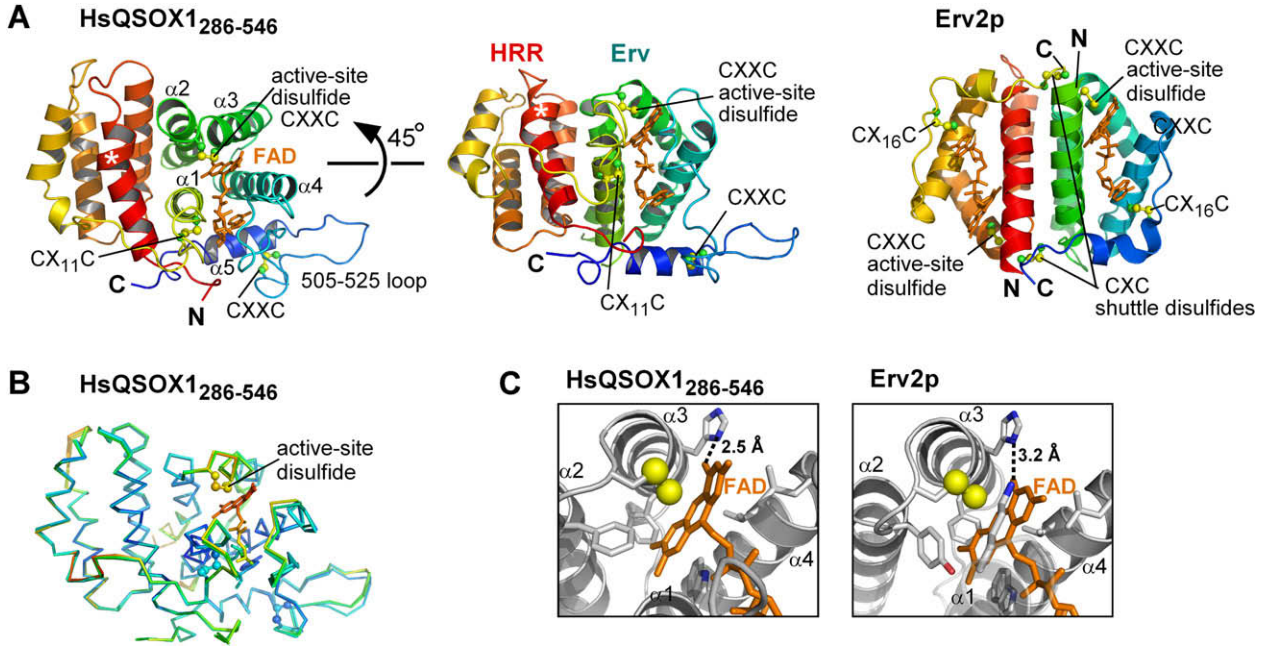

Fig. 2. Structure of $HsQSOX_{286-546}$ and comparison with a single-domain Erv enzyme. (A) Left, disulfide motifs (shown as balls-and-sticks) and the helices in the FAD binding domain are labeled on a ribbon diagram of $HsQSOX_{286-546}$ (molecule C from the C222 structure). FAD is represented in orange sticks. The central panel shows the view obtained by rotating 45° around the horizontal axis. The structure of yeast Erv2p (PDB ID code 1JR8) [19] is shown on the right for comparison. The FAD binding domains of HsQSOX and Erv2p are very similar, and the HRR of QSOX appears to be a degenerate Erv sulfhydryl oxidase domain that packs against the active domain with similar geometry as seen in the Erv family dimers. An interesting helical turn containing an extra residue (~4.5 instead of the canonical ~3.6) in the HRR is labeled with a white asterisk (*). (B) Cα traces of the multiple copies of $HsQSOX_{286-546}$ in the C222 crystals (molecules A–C) are superposed and colored according to B factor (high = red, low = blue). The region of the active-site, including the isoalloxazine of the FAD, has relatively high mobility within the crystals. (C) The active-site regions of $HsQSOX_{286-546}$ and yeast Erv2p are shown. Amino acid side chains in stick representation contribute to the hydrophobic pocket in which the FAD isoalloxazine binds. Sulfurs in the active-site disulfides are shown as spheres at half their van der Waals radii. Helix α1 of Erv2p is semi-transparent so that the FAD isoalloxazine and the tryptophan residue against which it packs can be seen below it. The lysine side chain that points into the active-site of Erv2p and other Erv family sulfhydryl oxidases (but is not seen in the $HsQSOX_{286-546}$ fragment) is shown in the center of the Erv2p image.

(residues 505–525) projecting out of the $HsQSOX1_{286-546}$ structure upstream of helix α5 (Fig. 2A).

3.3. Structure of the QSOX helix-rich region

The HRR forms a compact four-helix bundle domain. When we superposed $HsQSOX1_{286-546}$ on other Erv family domains, we observed a remarkable correspondence between the helices of QSOX HRR and the second subunit of the Erv dimer (Fig. 2A, compare yellow/orange/red helical domains in central and right ribbon diagrams). Automated structure comparison [32] confirmed the similarity, listing an Erv family protein as the highest structural match to the HRR (*Z* score 6.0), after a de novo designed di-iron protein (*Z* score 6.2). Despite the similarity of the HRR to Erv domains in helix topology, the HRR lacks active-site cysteines as well as the residues that form the FAD binding motif of Erv enzymes [31]. Furthermore, the interhelical packing angles do not precisely match those of functional Erv domains. Other high-scoring structural matches to the HRR were hemerythrin (*Z* score 5.5) and cytochrome *c*′ (*Z* score 4.4), which, like the designed di-iron protein, bind other cofactors and not FAD.

4. Discussion

The carboxy-terminal portion of HsQSOX1, comprising the sulfhydryl oxidase active site, appears to be a product of domain duplication and fusion. The result is a pseudo-dimeric structure with remarkable similarity to the true dimers of Erv sulfhydryl oxidase enzymes. Only one of the "subunits" of the HsQSOX1 pseudo-dimer has retained activity as a sulfhydryl oxidase, however, and even this module depends for efficient catalysis on the presence of a functional PDI-like oxidoreductase domain at the QSOX amino terminus [13,23]. The redox-active disulfide in the QSOX amino-terminal domain may serve as the direct electron donor to the FAD-proximal cysteines, as illustrated in Fig. 1. It will be interesting to find out if the QSOX PDI-like domain also supplies the missing basic residue to stabilize an active-site thiolate in the Erv domain during catalysis.

Single-domain Erv sulfhydryl oxidases lack a PDI-like domain and thus naturally resemble the QSOX fragment structure presented herein (Fig. 2A). Like QSOX, though, many Erv enzymes also require multiple disulfides for catalysis. In addition to the FAD-proximal disulfide, Erv enzymes often contain, near one of the termini, an additional, "shuttle" disulfide in a $CX_{1-4}C$ motif that transfers electrons from substrate to the active site. The CXXC motif near the carboxy-terminus of QSOX was a candidate for such a role, but the $HsQSOX1_{286-546}$ structure shows this disulfide to be on the opposite side of the protein, 27 Å through the protein core and a greater distance circumferentially from the active site. Furthermore, this disulfide is functionally dispensable for QSOX oxidation of small molecule and model protein substrates in vitro [23]. Whether this conserved CXXC disulfide is redox-active in another capacity or has a structural role in QSOX enzymes remains to be determined, but it is not likely to serve as a shuttle to the active-site cysteines in a manner directly analogous to the single-domain Erv family proteins.

The HsQSOX1 HRR, which shows structural similarity both to the Erv family and to primitive oxygen and electron carrying

proteins such as hemerythrins and four-helix bundle cytochromes, underscores the versatility of this simple fold. It is interesting to note that hemerythrins coordinate two iron atoms using a series of amino acid side chains including five histidines. Histidines are also used to ligate heme in cytochromes. The consensus sequence for FAD binding by Erv domains contains a core di-histidine motif [31]. Though highly speculative, Erv enzymes, including QSOX, may share common origins with primordial metal-binding proteins.

5. Author contributions

A.A. prepared, purified, and crystallized the protein. A.A. and D.F. collected crystallographic data and solved the crystal structures. All authors discussed the results and contributed to the writing of the manuscript.

6. PDB accession codes

The atomic coordinates and structure factors have been deposited in the Protein Data Bank with the accession codes 3LLI and 3LLK.

Acknowledgement

This study was supported by the Israel Science Foundation and the Kimmelman Center for Macromolecular Assemblies.

References

[1] Frand, A.R. and Kaiser, C.A. (1998) The ERO1 gene of yeast is required for oxidation of protein dithiols in the endoplasmic reticulum. Mol. Cell 1, 161–170.
[2] Pollard, M.G., Travers, K.J. and Weissman, J.S. (1998) Ero1p: a novel and ubiquitous protein with an essential role in oxidative protein folding in the endoplasmic reticulum. Mol. Cell 1, 171–182.
[3] Tian, G., Xiang, S., Noiva, R., Lennarz, W.J. and Schindelin, H. (2006) The crystal structure of yeast protein disulfide isomerase suggests cooperativity between its active sites. Cell 124, 61–73.
[4] Coppock, D.L., Kopman, C., Scandalis, S. and Gilleran, S. (1993) Preferential gene expression in quiescent human lung fibroblasts. Cell Growth Differ. 4, 483–493.
[5] Coppock, D.L., Cina-Poppe, D. and Gilleran, S. (1998) The Quiescin Q6 gene (QSCN6) is a fusion of two ancient gene families: thioredoxin and ERV1. Genomics 54, 460–468.
[6] Antwi, K., Hostetter, G., Demeure, M.J., Katchman, B.A., Decker, G.A., Ruiz, Y., Sielaff, T.D., Koep, L.J. and Lake, D.F. (2009) Analysis of the plasma peptidome from pancreas cancer patients connects a peptide in plasma to overexpression of the parent protein in tumors. J. Proteome Res. 8, 4722–4731.
[7] Song, H., Zhang, B., Watson, M.A., Humphrey, P.A., Lim, H. and Milbrandt, J. (2009) Loss of Nkx3.1 leads to the activation of discrete downstream target genes during prostate tumorigenesis. Oncogene 28, 3307–3319.
[8] Tury, A., Mairet-Coello, G., Poncet, F., Jacquenard, C., Risold, P.Y., Fellmann, D. and Griffond, B. (2004) QSOX sulfhydryl oxidase in rat adenohypophysis: localization and regulation by estrogens. J. Endocrinol. 183, 353–363.
[9] Mairet-Coello, G., Tury, A., Esnard-Feve, A., Fellmann, D., Risold, P.-Y. and Griffond, B. (2004) FAD-linked sulfhydryl oxidase QSOX: topographic, cellular, and subcellular immunolocalization in adult rat central nervous system. J. Comp. Neurol. 473, 334–363.
[10] Chakravarthi, S., Jessop, C.E., Willer, M., Stirling, C.J. and Bulleid, N.J. (2007) Intracellular catalysis of disulfide bond formation by the human sulfhydryl oxidase, QSOX1. Biochem. J. 404, 403–411.
[11] Coppock, D.L. and Thorpe, C. (2006) Multidomain flavin-dependent sulfhydryl oxidases. Antiox. Redox Signal. 8, 300–311.
[12] Tury, A., Mairet-Coello, G., Esnard-Fève, A., Esnard-Fève, A., Benayoun, B., Risold, P.-Y., Griffond, B., Griffond, B. and Fellmann, D. (2006) Cell-specific localization of the sulphydryl oxidase QSOX in rat peripheral tissues. Cell Tissue Res. 323, 91–103.
[13] Raje, S. and Thorpe, C. (2003) Inter-domain redox communication in flavoenzymes of the quiescin/sulfhydryl oxidase family: role of a thioredoxin domain in disulfide bond formation. Biochemistry 42, 4560–4568.
[14] Deponte, M. and Hell, K. (2009) Disulphide bond formation in the intermembrane space of mitochondria. J. Biochem. 146, 599–608.
[15] Hakim, M. and Fass, D. (2010) Cytosolic disulfide bond formation in cells infected with large nucleocytoplasmic DNA viruses, Antiox. Redox Signal. (2010), [Epub ahead of print].
[16] Hoober, K.L., Joneja, B., White 3rd, H.B. and Thorpe, C. (1996) A sulfhydryl oxidase from chicken egg white. J. Biol. Chem. 271, 30510–30516.
[17] Hoober, K.L. and Thorpe, C. (1999) Egg white sulfhydryl oxidase: kinetic mechanism of the catalysis of disulfide bond formation. Biochemistry 38, 3211–3217.
[18] Hoober, K.L., Sheasley, S.L., Gilbert, H.F. and Thorpe, C. (1999) Sulfhydryl oxidase from egg white: a facile catalyst for disulfide bond formation in proteins and peptides. J. Biol. Chem. 274, 22147–22150.
[19] Gross, E., Sevier, C.S., Vala, A., Kaiser, C.A. and Fass, D. (2002) A new FAD-binding fold and intersubunit disulfide shuttle in the thiol oxidase Erv2p. Nat. Struct. Biol. 9, 61–67.
[20] Wu, C.K., Dailey, T.A., Dailey, H.A., Wang, B.C. and Rose, J.P. (2003) The crystal structure of augmenter of liver regeneration: a mammalian FAD-dependent sulfhydryl oxidase. Protein Sci. 12, 1109–1118.
[21] Vitu, E., Bentzur, M., Lisowsky, T., Kaiser, C.A. and Fass, D. (2006) Gain of function in an ERV/ALR sulfhydryl oxidase by molecular engineering of the shuttle disulfide. J. Mol. Biol. 362, 89–101.
[22] Hakim, M. and Fass, D. (2009) Dimer interface migration in a viral sulfhydryl oxidase. J. Mol. Biol. 391, 758–768.
[23] Heckler, E.J., Alon, A., Fass, D. and Thorpe, C. (2008) Human quiescin-sulfhydryl oxidase, QSOX1: probing internal redox steps by mutagenesis. Biochemistry 47, 4955–4963.
[24] Ostrowski, M.C. and Kistler, W.S. (1980) Properties of a flavoprotein sulfhydryl oxidase from rat seminal vesicle secretion. Biochemistry 19, 2639–2645.
[25] Van Duyne, G.G., Standaert, R.F., Karplus, P.A., Schreiber, S.L. and Clardy, J. (1993) Atomic structures of the human immunophilin FKBP-12 complexes with FK506 and rapamycin. J. Mol. Biol. 229, 105–124.
[26] Otwinowski, Z. and Minor, W. (1997) Processing of X-ray diffraction data collected in oscillation mode. Methods Enzymol. 276, 307–326.
[27] Adams, P.D., Grosse-Kunstleve, R.W., Hung, L.-W., Ioerger, T.R., McCoy, A.J., Moriarty, N.W., Read, R.J., Sacchettini, J.C., Sauter, N.K. and Terwilliger, T.C. (2002) PHENIX: building new software for automated crystallographic structure determination. Acta Cryst. D58, 1948–1954.
[28] Emsley, P. and Cowtan, K. (2005) Coot: model-building tools for molecular graphics. Acta Crystallogr. D 60, 2126–2132.
[29] McCoy, A.J., Grosse-Kunstleve, R.W., Adams, P.D., Winn, M.D., Storoni, L.C. and Read, R.J. (2007) *Phaser* crystallographic software. J. Appl. Cryst. 40, 658–674.
[30] Brunger, A.T. et al. (1998) Crystallography & NMR system: a new software suite for macromolecular structure determination. Acta Crystallogr. D 54, 905–921.
[31] Fass, D. (2008) The Erv family of sulfhydryl oxidases. Biochim. Biophys. Acta 1783, 557–566.
[32] Holm, L., Kaariainen, S., Rosenstrom, P. and Schenkel, A. (2008) Searching protein structure databases with DaliLite v.3. Bioinformatics 24, 2780–2781.
[33] Weiss, M.S. (2001) Global indicators of X-ray data quality. J. Appl. Crystallogr. 34, 130–135.